International Symposium of Research Students on Materials Science and Engineering
December 20-22, 2004, Chennai, India
Department of Metallurgical and Materials Engineering, Indian Institute of Technology Madras

ZIRCONIUM BASED BULK METALLIC GLASS/ TUNGSTEN FIBRE COMPOSITE- FABRICATION AND CHARACTERIZATION

S. Neogy[1], A. Mukherjee[2], B. Ashwini[3], D. Srivastava[1], R. T. Savalia[1], G. K. Dey[1], N. Venkatraman[4], P. K. De[1]

[1]*Materials Science Division, Bhabha Atomic Research Centre, Mumbai 400 085, India*
[2]*Materials Processing Division, Bhabha Atomic Research Centre, Mumbai 400 085, India*
[3]*Metallurgical & Materials Engineering Department, Indian Institute of Technology, Madras*
[4]*Defence Metallurgical Research Laboratory, Kanchanbagh, Hyderabad 500 058, India*

ABSTRACT

The aim of the present work was to fabricate and characterize a composite consisting of Zr based bulk metallic glass as the matrix and W fibres as the reinforcement. This kind of composite because of its very high impact toughness has got widespread applications including strategic areas. The glass forming alloy taken for this purpose was $Zr_{52}Ti_6Al_{10}Cu_{18}Ni_{14}$ (at%) because of its high glass forming ability (GFA). W was selected as the reinforcing medium because of its high melting point and high strength. The composite was fabricated in a unique way where a preform of W wires was made and the glass forming alloy was vitrified with this preform as reinforcement using the copper mold casting technique The composite was characterized using optical microscopy and EPMA studies. Compression testing was done to evaluate the mechanical properties of the composite.

Keywords: Zirconium, bulk metallic glass, tungsten, fibre, composite.

1. INTRODUCTION

Metallic glasses have many useful and unusual properties because of their noncrystalline atomic arrangement[1]. The necessity of rapid solidification at cooling rates of 10^5K/sec. or higher for their production has restricted their geometry to thin ribbons and prevented their application to many areas despite their excellent properties. However, it has been shown in recent investigations that many Zr based multicomponent alloys can be obtained in glassy state by cooling at much lower rates typically 10^2 to 10^3 K/sec[2, 3]. This has enabled production of these alloys in the glassy state in bulk. By now bulk metallic glasses have been made in Mg, Ln, Zr, Fe, Pd-Cu, Pd-Fe, Ti and Ni- based alloys. Production of these glasses in bulk has opened avenues for their application in many areas where their excellent mechanical properties and corrosion resistance can be exploited. The bulk amorphous alloys exhibit higher fracture stress combined with higher hardness and lower Young's modulus than those of any crystalline alloy. They have high bending and flexural strength values, which are 2. 0 to 2.5 times higher than those for crystalline Zr- and Ti-based alloys. The Zr based amorphous alloys have simultaneously high tensile strength, high hardness, high bending strength, high fracture toughness, high impact fracture energy, high fracture strength and good corrosion resistance[4]. Upon yielding, metallic glasses however form localized shear bands. The localization of shear is associated with the absence of strain hardening (work hardening) mechanism, possible strain softening and thermal softening during adiabatic heating of material. Within bands, one observes large local plastic strain. Unfortunately, without geometrical confinement, failure occurs along a single band. The plane strain fracture toughness K_{IC}=20-55MNm$^{1/2}$ of Vitreloy 1

$[(Zr_3Ti)_{0.55}(Cu_5Ni_4)_{0.225}Be_{0.225}]$ suggests the existence of a significant plastic zone that screens crack tip. But in tensile loading there is little global plasticity whereas crystalline metals exhibit significant plastic yielding and has plane strain fracture toughness, K_{IC}=50-100 $MNm^{1/2}$. Role of geometry in the deformation behaviour is important. Geometrical confinement of shear bands can enhance overall plasticity. In uniaxial tensile tests, shear bands are always unconfined. Failure is invariably along a single or small number of shear bands. The possibility of shear band confinement under tension was nicely demonstrated by Courtney, who fabricated laminated composite specimen consisting of a layer of metallic glass bonded between two ductile metal layers. Shear bands formed in the glassy layer are blunted by the ductile layers. Stress is redistributed at the blunting site and multiple shear bands are formed. Single shears band thus no longer leads to failure. Courtney observed a high density of multiple shear bands "trapped" between the ductile metal layers. Overall plastic tensile strain that could be achieved was 10%[4].

In an effort to overcome the problem of limited plasticity and to develop engineering applications, recent efforts have been focused on developing bulk metallic glass composite. A variety of composite materials have been formed by the direct introduction of reinforcing crystalline solid phase into the glass forming melt[4]. The melt is cooled to produce a metallic glass-matrix composite structure. For a good composite material the fibres must have high strength and high elastic modulus and the matrix must be ductile and non reactive with the fibres. The fibres may be long and continuous, or they may be discontinuous. In fibre strengthening the high modulus fibres carry essentially the entire load. The matrix serves to transmit the load to the fibres, to protect fibres from surface damage, and to separate the individual fibres and blunt cracks which arise from fibre breakage. Because the fibres and the matrix have quite different elastic moduli a complex stress distribution is developed when a composite body is loaded uniaxially in the direction of the fibres.

Composite with bulk metallic glass as the matrix and tungsten fibre as the reinforcing medium have been found to have special properties. Such a composite has very high impact strength and is especially suitable for application as an armor penetrator in various types of shells used in the defense. When the composite is subjected to uniaxial compression and tension, one finds that the overall composite exhibits enhanced plastic strain to failure. Deformation occurs, as in glass by the propagation of localized shear bands (at an angle of 45^0 to the compressive axis). But the interaction of shear bands with the W wires results in the generation of multiple shear bands, which are confined by their interaction with the wires. The failure of tungsten containing composite in compression by formation of localized shear bands is of practical interest. This mode of failure is greatly desired in the design of W- based armor piercing kinetic energy penetrators. Ballistic testing of W/BMG composite has indeed shown that the performance is greatly enhanced in comparison to ordinary crystalline W alloys. This can be directly attributed to the influence of metallic glass matrix in inducing localized shear deformation. This type of deformation leads to 'self-sharpening' behavior of the penetrator[4].

Fabrication of W fibre reinforced bulk metallic glass composite has been tried in many ways. In one of those techniques a composite of W fibers and Vitreloy 1 was made by infiltration technique where the fibres were bundled together and then infiltrated by the capillary flow of the molten alloy under gravity. The main disadvantage of this technique lies in the material of the enclosure which is used to hold the bundles together. In general the enclosure is made up of either silica or steel which (i) lowers the cooling rate thereby affecting the glass forming ability and (ii) contaminates the melt either with oxygen (from silica) or with iron, carbon (from steel). In contrast the copper mold casting technique (details of which are given in the experimental section) which has been used in the present study does not lead to all these problems.

2. EXPERIMENTAL PROCEDURE

Crystal bar zirconium and high purity elements were melted in the right proportion in a vacuum arc furnace for preparing the glass-forming alloy. Repeated melting of the arc-melted button was carried out for composition homogenization. The alloy was obtained in the bulk amorphous form by copper mold casting technique where small pieces of the arc melted button were used to produce bulk metallic glass rods by induction melting these in quartz crucible and injecting the melt in a copper mold under protective argon atmosphere (Fig. 1). The diameter of the mold cavity was 6 mm and the length was 55 mm. In composite making a preform of W wires was first made. A wire holding copper disc (copper guiding block) was made with the geometry as shown in Fig. 2. The idea behind using copper was to have high cooling rate and also to avoid contamination in the melt. Tungsten wires of 1.38 mm diameter were cut using a shear cutter and then embedded in the hexagonally arranged holes as shown in Fig. 3. This arrangement was carefully put inside the copper mold and the same procedure which was followed for making the bulk glass was repeated to give the composite (Fig. 4). The volume fraction of the reinforcing tungsten fibres was 31%.

The arc melted and the bulk glass microstructures of the alloy have been characterized by optical microscopy, X-Ray diffraction, electron probe micro analysis (EPMA) and conventional and high-resolution transmission electron microscopy (TEM). The composite was characterized by optical microscopy and EPMA studies. Compression testing was carried out to evaluate the mechanical properties of the bulk glass as well as that of the composite.
In optical microscopy the etching of the samples were performed by swabbing the surface of the samples with cotton dipped in a solution having a composition of 50 ml water, 45 ml HNO_3 and 5 ml HF. Etching time was approximately 10 to 15 sec. The optical samples were subjected to composition analysis in CAMECA SX 100 Electron Probe Micro Analyzer. TEM specimens were prepared by twinjet electropolishing in an electrolyte having a composition of 80 % methanol and 20% perchloric acid. The bath temperature was kept at -50^0 C and voltage was maintained at 25V. Conventional transmission electron microscopy was carried out in a JEOL 2000 FX transmission electron microscope and high resolution transmission electron microscopy (HRTEM) was carried out in JEOL 3010 transmission electron microscope.

3. RESULTS AND DISCUSSION

3.1 Arc melted microstructure of the glass forming alloy

Optical microscopy of the arc melted alloy button was carried out. The microstructure revealed the presence of isolated dendrites (Fig. 5(a)). The presence of secondary and tertiary dendrites besides the primary dendrites could also be seen in this micrograph.

The arc melted sample was also subjected to electron probe microanalysis. Fig. 5(b) shows the back scattered electron image obtained in EPMA. Similar to the optical micrograph isolated dendrites could be seen here also but compositionally the microstructure was found to consist of many phases. Phase 1 constituted the isolated dark phase which was highly irregular in shape and was of varying sizes. They joined locally to give larger dimensions. This phase also showed severe branching into secondary and tertiary arms. A set of fine white lamellae constituted the phase 2. The size and shape of this phase was found to be more or less consistent. The formation of lamellae could be due to micro segregation during the growth of dendrites. The matrix between the dark phase and the white lamellae (phase 3) was found to be different from the bulk matrix phase (phase 5) where dendrites have not grown. The microstructure also revealed the presence of some gray lamellae (phase 4) within the bulk matrix phase. The composition of each of the above phases is given in a tabular form in Table. 1.

X-Ray diffraction analysis of the arc melted microstructure was also carried out to identify the crystalline phases formed in the arc melted alloy button as these phases would be competing with glass formation in this alloy. The diffractogram obtained is shown in Fig. 5(c). The major peaks of the XRD pattern were indexed to indicate the phases and the planes from which diffraction has occurred. Zr_5Al_3 and Zr_2Cu were found to be the dominant phases. The initial broad peak was from the glass plate on which the sample was mounted in the diffractometer. Fig. 5(d) shows a bright field TEM micrograph where a dark lamellar phase indicative of the dendritic arm could be seen embedded in a bright phase indicative of the matrix phase. The length and width of the dark lamellae was in the range of 3 to 5 μm and 0.5 to 2 μm respectively. Selected area electron diffraction (SAED) analysis (Fig. 5(e)) from the bright phase confirmed that it is Zr_2Cu type.

3.2 Bulk glass microstructure

The microstructure of the as cast bulk metallic glass was found to be fully amorphous under conventional microscopy, electron and x-ray diffraction studies. Amorphous nature of the microstructure has been confirmed by the SAED pattern given in Fig. 6. However, high resolution transmission electron microscopy (HRTEM) showed the presence of very few, very small (3 - 4 nm) crystalline regions which could be called as quenched-in nuclei of crystalline phases. An amorphous matrix separated such regions from one another. The presence of such quenched-in nuclei of crystalline phases gets revealed in a HRTEM micrograph in the form of lattice fringes sparsely distributed in the matrix. In the process of crystallization of the amorphous phase these quenched-in nuclei have been found to play an important role[5, 6]. The absence of interfaces such as twins or stacking faults inside these nuclei indicated that these interfaces do not develop during the solidification process.

3.3 Microstructure of the composite

The composite was characterized by optical microscopy where the position of the six wires could be clearly seen. EPMA studies were done on the sample to check whether any chemical reaction has occurred at the fiber/matrix interface. However there was no chemical reaction at the fiber/matrix interface. The X-ray image of fiber and BMG matrix with W L_α, Zr L_α and Al K_α as shown in Figs. 7(a), 7(b) and 7(c) respectively suggested that no transfer of elements have occurred across the interface.

3.4 Mechanical properties

The dynamic compression testing results of the bulk metallic glass (BMG) and bulk glass matrix/ tungsten fibre composite (BMG-COMP) are shown in Fig. 8. The BMG has slightly greater fracture stress (1904 MPa) as compared to BMG-COMP (1783 MPa) but the plastic strain to failure for BMG-COMP (0.558) is one order of magnitude higher than for BMG (0.06). This suggested that metallic glass reinforced with tungsten fibres show inhibited shear band formation, resulting in the generation of multiple shear bands and substantial plastic deformation.

4. CONCLUSIONS

1. Microstructure of the arc melted $Zr_{52}Ti_6Al_{10}Cu_{18}Ni_{14}$ alloy has been characterized by optical, EPMA and TEM studies. The microstructure was mostly dendritic with fine white lamellae in the interdendritic regions. The white phase (lamellae) has been found to be Zr_2Cu.
2. The amorphous form of the alloy was studied using TEM and it showed the presence of quenched-in nuclei of 3-4 nm size embedded in the amorphous matrix.

3. The composite of tungsten wires preform and bulk glass was fabricated by copper mold casting technique and was characterized using optical and EPMA. Compression testing was done to find the strength of the composite.
4. The microstructural observation of the composite suggested that the wires were uniformly distributed and there was no chemical reaction at the interface of tungsten wires and bulk glass.
5. The results of dynamic compression testing of bulk glass (BMG) and BMG-W fibre composite showed that BMG has slightly greater fracture stress (1904 MPa) compared to composite (1783 MPa) but the plastic strain to failure for the composite (0.558) was one order of magnitude higher than for BMG (0.06). This suggested that metallic glass reinforced with tungsten fibres show inhibited shear band formation, resulting in the generation of multiple shear bands and substantial plastic deformation.

REFERENCES

1. Suryanrayana C, *Int. Mat. Rev.* **40** (1995) 41.
2. Inoue A, *Bulk Amorphous Alloys*, Trans Tech Publications, Zuerich (1998-99).
3. Inoue A, *Acta Mater.* **48** (2000) 279.
4. Johnson W L, *MRS Bulletin.* (Oct. 1999) p 42.
5. Dey G K, Savalia R T, Baburaj E G, and Banerjee S, *J. Mater. Res.* **13** (1998) 504.
6. Banerjee S, Savalia R T, and Dey G K, *Mat. Sci and Engg.* A. **304** (2001) 26.

TABLES

Table 1: Compositions (in at %) of various phases as obtained in EPMA study.

Composition (at%)	Phase 1 Dark phase	Phase 2 White lamellae	Phase 3 Matrix	Phase 4 Gray lamellae	Phase 5 General matrix	Alloy composition
Al	16.20873	2.01185	8.94901	12.75011	9.65548	10.00
Ti	12.12966	3.30119	2.88809	9.17092	6.18996	6.00
Ni	12.52526	8.48947	15.80929	13.94106	13.60493	14.00
Cu	18.98692	23.18027	15.42049	17.74989	17.85752	18.00
Zr	40.14943	63.01723	56.93312	46.38723	52.69211	52.00

FIGURES

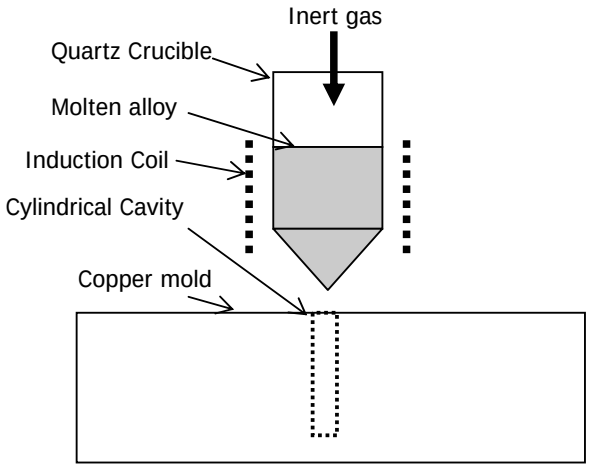

Fig. 1 Schematic diagram showing the set up for bulk metallic glass fabrication.

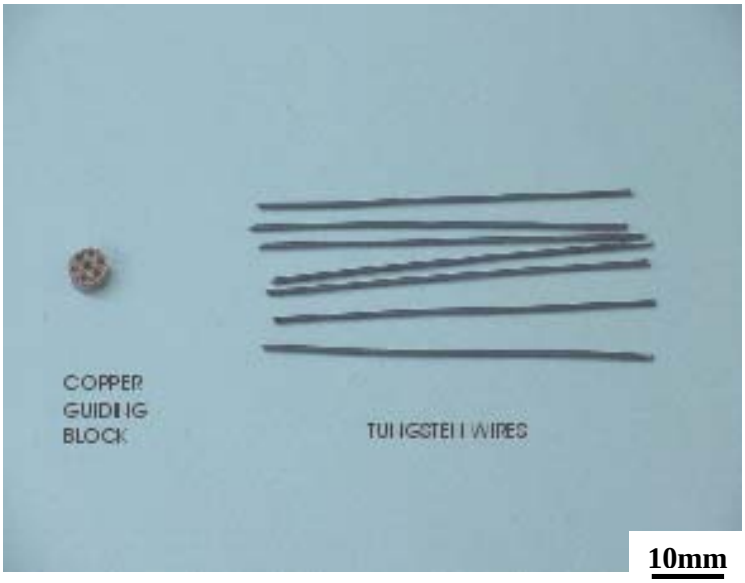

Fig. 2 Photograph showing copper guiding block and tungsten fibres.

Fig. 3 Photograph showing the preform of tungsten wires.

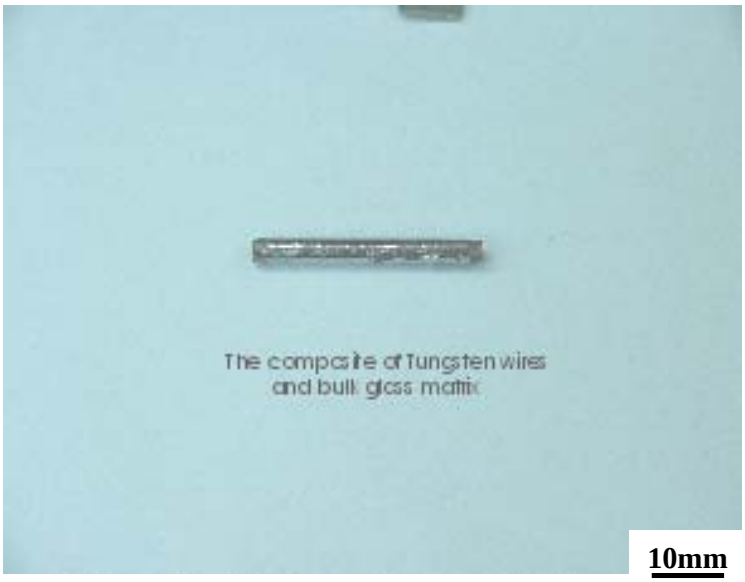

Fig. 4 Photograph showing bulk metallic glass/ tungsten fibre composite.

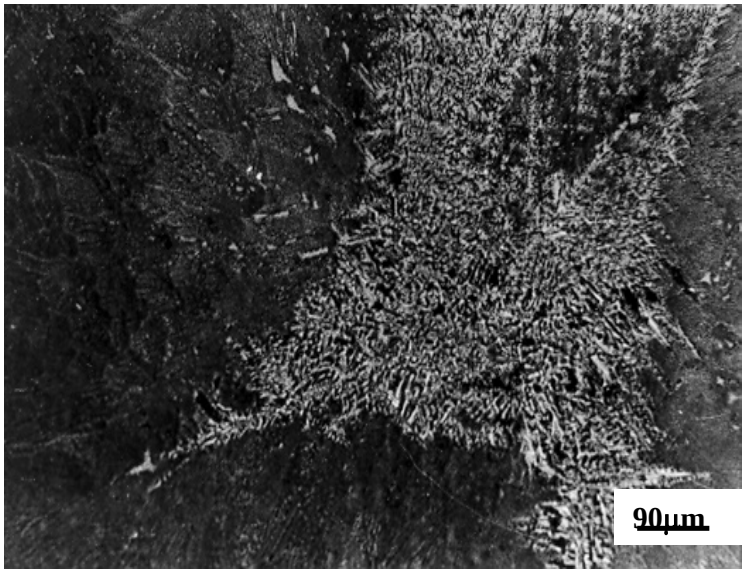

Fig. 5(a) Optical micrograph showing dendritic microstructure of the arc melted alloy button

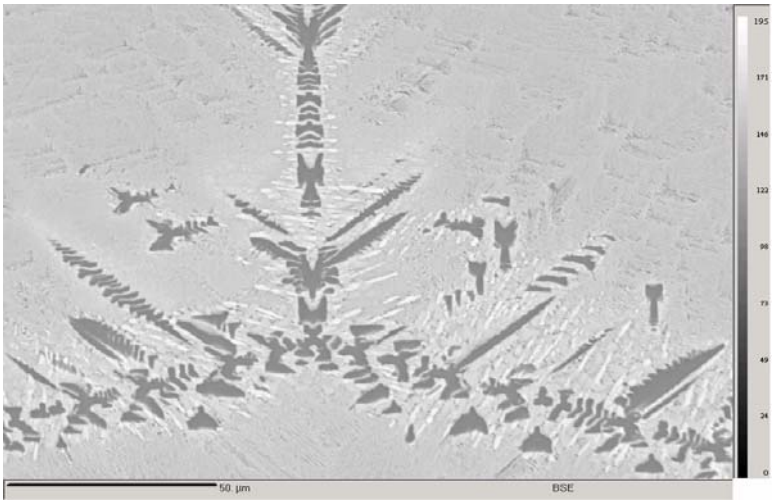

Fig. 5(b) Back scattered electron image of the arc melted microstructure of the glass forming alloy.

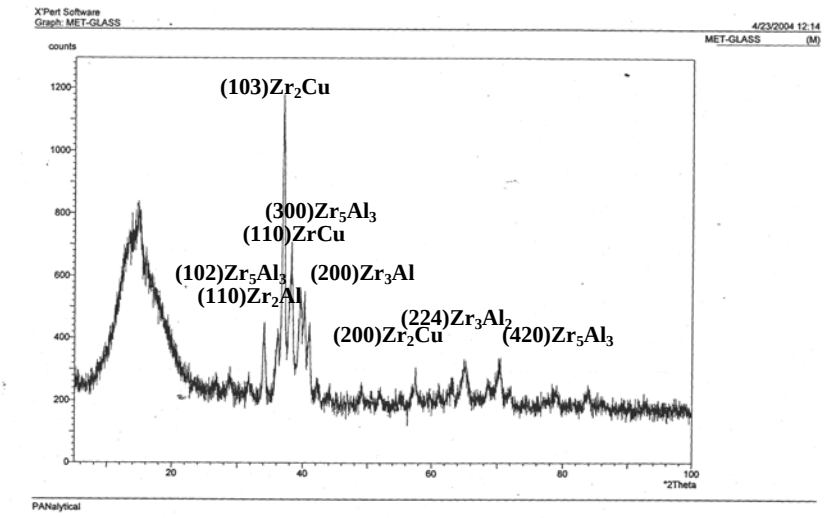

Fig. 5(c) X-Ray diffractogram obtained from the arc melted alloy button.

Fig. 5(d) Bright field TEM micrograph showing the microstructure of the arc melted alloy button.

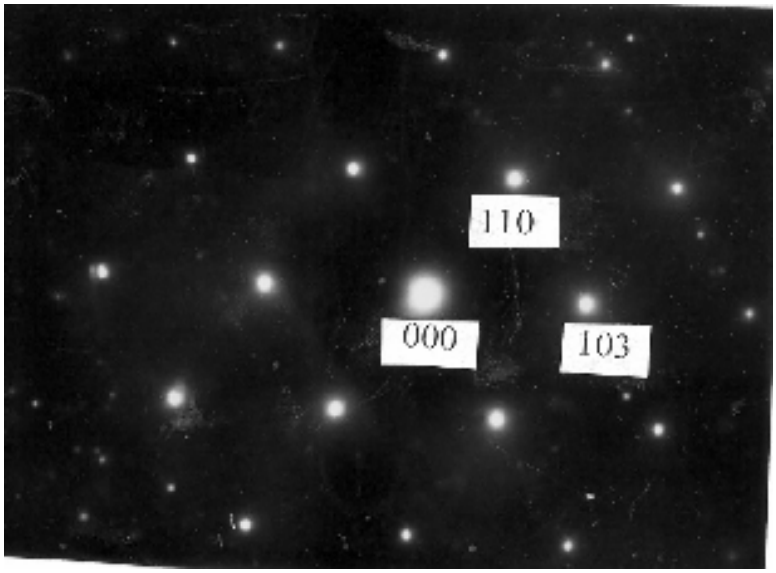

Fig. 5(e) SAED pattern obtained from the Zr_2Cu phase.

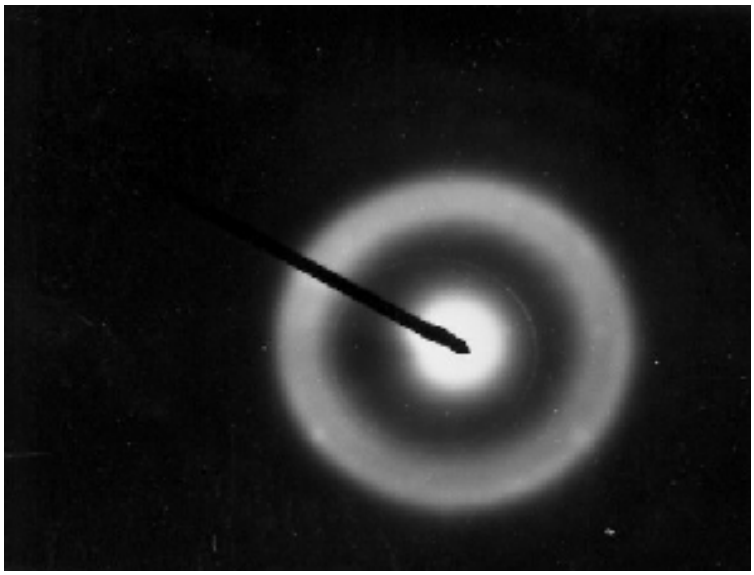

Fig. 6 SAED pattern showing the amorphous nature of the bulk glass microstructure.

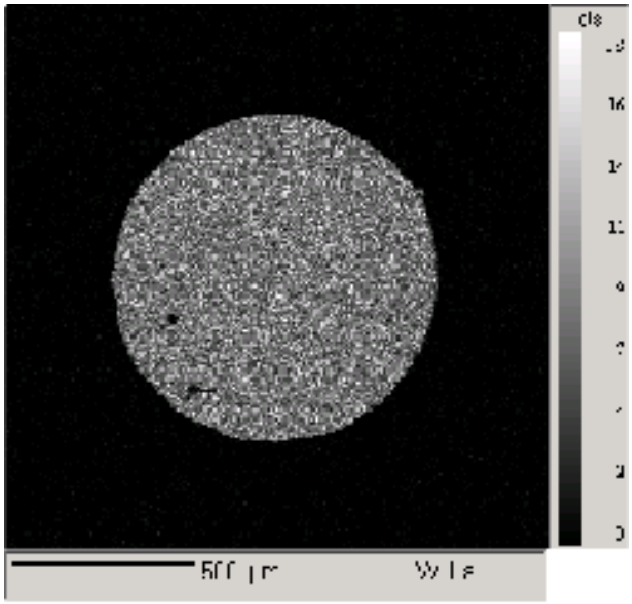

Fig. 7(a) X-ray image of fiber and BMG matrix with W L_{α}.

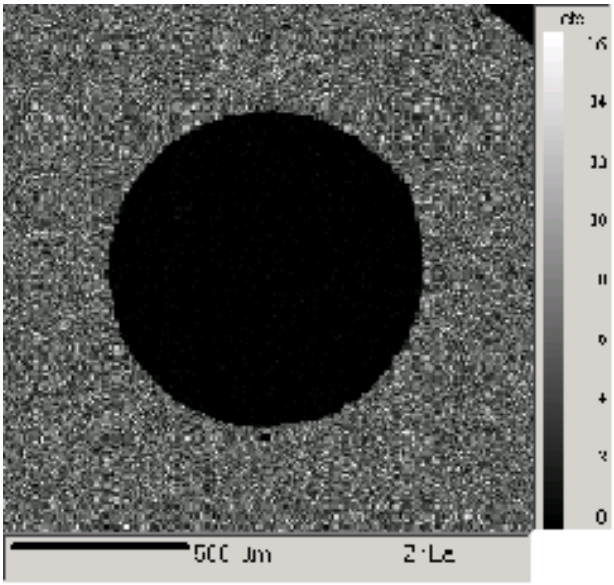

Fig. 7(b) X-ray image of fiber and BMG matrix with Zr L_{α}.

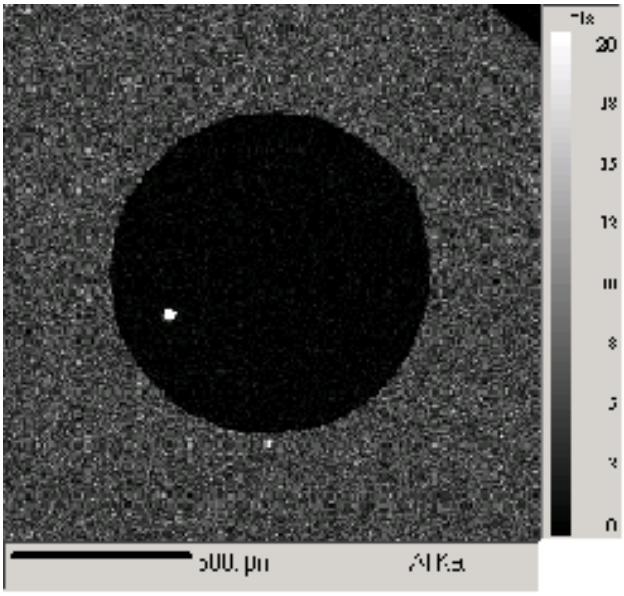

Fig. 7(c) X-ray image of fiber and BMG matrix with Al K_{α}.

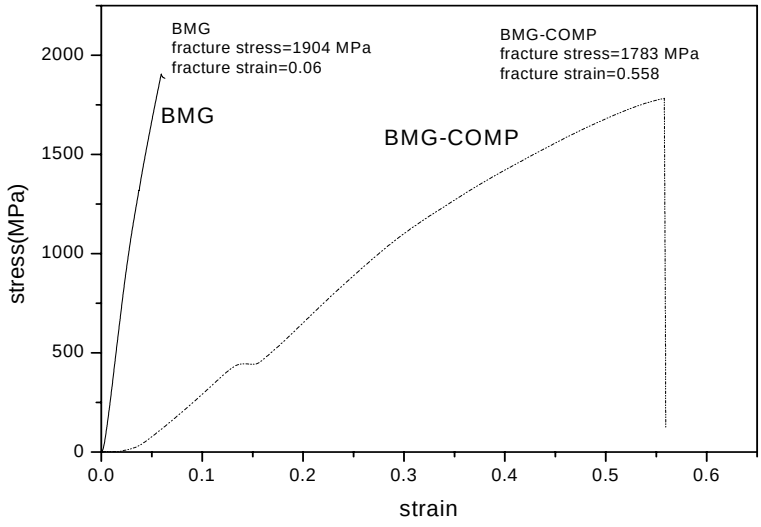

Fig. 8 Stress-strain plots showing the dynamic compression testing results of the bulk metallic glass (BMG) and bulk glass matrix/ tungsten fibre composite (BMG-COMP)